*** Manuscript [Word or (La)TeX]**

A quantile-quantile plot based pattern matching for defect detection

by

Du-Ming Tsai, Cheng-Hsiang Yang
Department of Industrial Engineering & Management
Yuan-Ze University, Taiwan, R.O.C.

Correspondence:

Du-Ming Tsai
Department of Industrial Engineering & Management
Yuan-Ze University
135 Yuan-Tung Road
Nei-Li, Tao-Yuan
Taiwan, R.O.C.

Tel: +886-3- 4638800 Ext. 507
Fax: +886-3- 4638907
E-mail: iedmtsai@saturn.yzu.edu.tw

A quantile-quantile plot based pattern matching for defect inspection

ABSTRACT

Pattern matching has been used extensively for many machine vision applications such as optical character recognition, face detection, object detection, and defect detection. The normalized cross correlation (NCC) is the most commonly used technique in pattern matching. However, it is computationally intensive, sensitive to environmental changes such as lighting and shifting, and suffers from false alarms for a complicated image that contains partial uniform regions. In this paper, a pattern matching scheme based on the quantile-quantile plot (Q-Q plot) is proposed for defect detection applications. In a Q-Q plot, the quantiles of an inspection image are plotted against the corresponding quantiles of the template image. The p-value of Chi-square test from the resulting Q-Q plot is then used as the quantitative measure of similarity between two compared images. The quantile representation transforms the 2D gray-level information into the 1D quantile one. It can therefore efficiently reduce the dimensionality of the data, and accelerate the computation. Experimental results have shown that the proposed pattern matching scheme is computationally fast and is tolerable to minor displacement and process variation. The proposed similarity measure of p-value has excellent discrimination capability to detect subtle defects, compared with the traditional measure of NCC. With a proper normalization of the Q-Q plot, the p-value measure can be tolerable to moderate light changes. Experimental results from assembled PCB (printed circuit board) samples, IC wafers, and LCD (liquid crystal display) panels have shown the efficacy of the proposed pattern matching scheme for defect detection.

Keywords: Defect detection; Pattern matching; Quantile-quantile plot; Similarity measure

1. INTRODUCTION

Template matching has been a commonly used technique for object detection (Ooi and Rao, 1991; Ratan *et al*., 2000; Tsai and Tsai, 2002), Face detection (Brunelli and Poggio, 1993; Grudin, 2000), and industrial inspections of printed circuit boards (Kim *et al*., 1996), surface-mounted devices (Gallegos *et al*., 1996), wafers (Cai *et al*., 1994), printed-character quality (Chang *et al*., 2001), fabrics (Yazdi and King, 1998) and ceramic tiles (Costa and Petrou, 2000). In object detection applications, it finds a pattern in the scene image by sliding the window of a reference template in a pixel-by-pixel basis, and computing the degree of similarity between image window and reference template. The peak of the measured similarity values indicates an instance of the template in the scene image. In defect inspection applications, the similarity measure between two windowed subimages at coincident locations in their respective inspection image and faultless template image is calculated, and the process is repeated for all pixels in the whole image. A small similarity value below some predetermined threshold indicates the presence of a defect.

The measure of similarity in template matching is commonly given by the normalized cross correlation (NCC). The traditional NCC that directly works on 2D gray-level images does not meet speed requirements for industrial applications. Furthermore, it is not highly responsive to the changes of two compared images and, therefore, cannot effectively discriminate the difference between faultless and defective regions in an inspection image. In order to alleviate the drawback of long processing time in template matching, the coarse-to-fine and multi-resolution search approaches (Gross and Rosenfeld, 1987; Penz *et al*., 1999; Bonmassar and Schwartz,

1998; Tsai and Chiang, 2002) have been widely used to reduce computational burden. Such algorithms first scan the image quickly and find all promising areas in the rough resolution, and then search for more accurate patterns and locations in the fine resolution. Lewis (2003) presented an algorithm that improves the calculation of the NCC for object detection by using precomputed sum tables. Tsai and Lin (2003) further extended Lewis' sum table approach for defect detection. Tsai *et al*. (2003) evaluated the use of the NCC for defect detection in complicated images. They pointed out that the NCC in gray-level images may result in false alarms for two compared images that contain uniform patterns. The detectability of NCCs in monochrome and color images, and the effect of image smoothing were empirically evaluated. They reported that the NCC in a smoothed color image can alleviate false alarms in defect detection applications. However, the discrimination ability for subtle defects remains a problem of NCC-based methods.

Our work has been motivated by a need to develop an efficient and effective similarity measure that can be significantly responsive to the degree of difference between two compared images. In this paper, a pattern matching scheme based on the quantile-quantile plot (Q-Q plot) is proposed for defect detection applications. In a Q-Q plot, the quantiles of the inspection image are plotted against the corresponding quantiles of the template image. If both compared images are identical, each pair of corresponding quantiles would plot on a straight line with slope 1 through the origin. The p-value of Chi-square test from the resulting Q-Q plot is then used as the quantitative measure of similarity between the two compared images. The quantile representation transforms the 2D gray-level information into the 1D quantile one. It can therefore efficiently reduce the dimensionality of the data, and accelerate the computation. The proposed similarity measure of p-value has excellent

discrimination capability to detect subtle defects, compared with the traditional measure of NCC. With a proper normalization of the Q-Q plot, the p-value measure can be tolerable to moderate light changes. The proposed pattern matching scheme is computationally fast and is insensitive to minor displacement and process variation.

This paper is organized as follows: Section 2 first describes the construction of a quantile-quantile plot, and interprets the shapes of gray-level distributions of various image contents in the plot. Then the p-value used as a quantitative measure of similarity between two compared images in the Q-Q plot is presented. Section 3 discusses the experimental results from test samples of assembled PCBs (printed circuit boards), IC wafers and LCD (liquid crystal display) panels. The paper is concluded in Section 4.

2. DEFECT DETECTION USING Q-Q PLOTS

2.1 The Q-Q plot

The quantile-quantile plot is traditionally a graphical technique for determining if two data sets come from populations with a common distribution in the context of statistics (NIST/SEMA TECH, 2004). Let $F(x)$ be the cumulative distribution that the continuous random variable X will have taken on a value no larger than the number x, i.e.,

$$F(x) = P(X \leq x) \tag{1}$$

The q-quantile of $F(x)$ is that number x_q such that $F(x_q) = q$. If F^{-1} denotes the inverse of $F(x)$, then $x_q = F^{-1}(q)$. For a continuous data set, the cumulative density function $F(x)$ is continuous and strictly increasing so that $F^{-1}(q)$ is uniquely defined. If two compared data sets come from a population with the same distribution, the points of paired quantiles will fall on a straight line with slope 1 through the origin in the plot. With the aid of Q-Q plots, we can then assess the similarity between two compared images. In gray-level images, the Q-Q plot is a graph of the q_i-quantile of the gray-level distribution $F_T(x)$ of the template image *T*, namely,

$$x_{q_i}^T = F_T^{-1}(q_i) \tag{2}$$

versus the q_i-quantile of the gray-level distribution $F_I(x)$ of the inspection image *I*, namely

$$x_{q_i}^I = F_I^{-1}(q_i) \tag{3}$$

For each quantile level q_i, a point of paired quantiles with coordinates $(x_{q_i}^I, x_{q_i}^T)$ is generated in the Q-Q plot. If both images are exactly the same, each pair of corresponding quantiles will follow an upward linear trend, with unit slope through the origin. There will be departures from the 45° reference line for two dissimilar images. The greater the departure from this reference line (or the greater the non-linearity of the resulting graph) in the plot, the greater the evidence of heterogeneity.

The Q-Q plot of two digital images can be constructed as follows. Let $m \times n$

be the selected window size for comparison, and $[0, L_{\max}]$ the range of gray levels. The probability of a gray level l in the window is given by

$$P_r(l) = \frac{h(l)}{m \cdot n} \quad , \quad l = 0,1,2,\ldots,L_{\max} \tag{4}$$

where $h(l)$ is the gray-level histogram in the window.

To produce a Q-Q plot in a traditional procedure, one needs first to sort the observed data points into ascending order so that the corresponding q-quantile variable x_q can be determined for each quantile level q. The sorting procedure is computationally intensive. Fortunately, the integer variables of gray levels $l's$ in a digital image are inherently arranged in increasing order. The discrete cumulative distribution function $\hat{F}(l)$ can then be easily calculated by

$$\hat{F}(l) = \sum_{i=0}^{l} P_r(i) \,, \quad l = 0,\ 1,\ 2,\ldots,L_{\max} \tag{5}$$

Given a percentage step Δq , we can construct K points of paired quantiles in the Q-Q plot, where

$$K = \left[\frac{1}{\Delta q} \right]$$

Hence, the quantile level q_k is given by

$$q_k = k \cdot \Delta q \,, \quad k = 1,2,\ldots.,K$$

For each quantile level q_k, the associated gray level variable l_k can be derived from

$$\hat{F}(l_k) = \sum_{i=1}^{l_k} P_r(i) = q_k \tag{6}$$

Since the gray level probability function $P_r(i)$ is discrete, the resultant gray-level variable can be determined by

$$l_k = \boldsymbol{arg\ min}\left\{\hat{F}(l_k) - q_k,\ q_k - \hat{F}(l_k - 1)\right\} \tag{7}$$

where $\hat{F}(l_k) \geq q_k$ and $\hat{F}(l_k - 1) < q_k$.

Let l_k^T and l_k^I be the q_k-quantiles of the template image and the inspection image, respectively, $k = 1,2,\ldots,K$. Therefore, we can generate K points of paired quantiles, each of coordinates $\left(l_k^I, l_k^T\right)$, in the Q-Q plot. In this study, the percentage step Δq is fixed to be 0.05. A total of 20 points will be generated in the Q-Q plot. The quantile representation transforms the 2D gray-level image into the 1D quantile signal. For a window image of arbitrary size $m \times n$, the number of data points can be reduced from $m \cdot n$ to only 20 with a percentage step of 0.05.

In order to illustrate how Q-Q plots help assess the similarity (or lack thereof) between two compared images, Figures 1-4 demonstrate four test images and their corresponding graphs of Q-Q plots. Figures 1(a) and (b) show two uniform images for comparison. Figure 1(c) presents the resulting Q-Q plot, in which the points of paired quantiles are highly concentrated on the 45° reference line. Figures 2(a) and (b) present two heterogeneous images, and Figure 2(c) show the corresponding Q-Q plot. An S-shaped curve indicates lack of similarity between these two compared

images. Figures 3(a) and (b) illustrate two identical printed character images. The resulting Q-Q plot, as seen in Figure 3(c), shows that the pairs of quantiles lie very nearly along the 45° reference line. It suggests a strong similarity between these two samples. Figure 4(b) further demonstrates a defective version of the printed character image in Figure 3(a). The Q-Q plot of Figures 4(a) vs. 4(b) appears rather curve-shaped, and visibly indicates lack of similarity.

Q-Q plots are qualitative rather quantitative methods for the comparison of two data sets. In this study, the straightness of a Q-Q plot along the 45° reference line, i.e., the similarity measure between two compared images, are evaluated by calculating the p-value of Chi-square test and the correlation coefficient of the paired quantiles in the plot.

2.2 The similarity measures in Q-Q plots

When two compared images are resembled, their Q-Q plot follows an upward linear trend. The straightness of the Q-Q plot is measured either by the correlation coefficient or by the p-value of Chi-square test in the plot, which are defined as follows.

The correlation coefficient

The correlation coefficient for the Q-Q plot with data points $\left\{\left(l_k^I, l_k^T\right)\right\}_{k=1}^{K}$ is given by

$$r_Q = \frac{\sum_{k=1}^{K}\left(l_k^T - \bar{l}^T\right)\left(l_k^I - \bar{l}^I\right)}{\left[\sum_{k=1}^{K}\left(l_k^T - \bar{l}^T\right)^2 \cdot \sum_{k=1}^{K}\left(l_k^I - \bar{l}^I\right)^2\right]^{1/2}} \tag{8}$$

where $\bar{l}^T$ and $\bar{l}^I$ are the means of l_k^T's and l_k^I's, respectively. For two identical images in comparison, the resultant correlation coefficient r_Q for the Q-Q plot has a maximum value of unity. The value of r_Q is in the range between -1 and 1. In this study, we take only non-negative values of r_Q, i.e., $r_Q = \max\{0, r_Q\}$, since a negative value of r_Q indicates a poor match or a reversal of intensities between two compared images in the application of defect inspection.

The p-value

The p-value is often referred to as the observed level of significance to hypothesis test in statistics, which is the smallest level at which the null hypothesis can be rejected for a given set of data (Levine *et al.*, 2001). A large p-value approximate to unity indicates a strong similarity, whereas a small p-value close to zero suggests a strong heterogeneity between two compared samples. The p-value of Chi-square test for linear trend in a Q-Q plot is obtained by first calculating the Chi-square statistic for the two quantile data sets $\{ l_k^T \}_{k=1}^K$ and $\{ l_k^I \}_{k=1}^K$. Since the data may not be normally distributed, the Chi-square statistic is calculated by

$$\chi^2 = \sum_{k=1}^{K} \left(l_k^I - l_k^T \right)^2 / l_k^T \tag{9}$$

Then the p-value of the Chi-square distribution is given by

$$p = \int_{\chi^2}^{\infty} \frac{2^{-\upsilon/2}}{\Gamma(\upsilon/2)} x^{(\upsilon/2)-1} e^{-x/2} \, dx \tag{10}$$

where υ is the degree of freedom, and $\upsilon = K - 1$;

$\Gamma(\upsilon/2)$ is the Gamma function given by

$$\Gamma(\upsilon/2) = \int_0^\infty t^{(\upsilon/2)-1} e^{-t}\, dt \tag{11}$$

The digital computation of the p-value can be found in the reference (UCLA, 2003).

Table 1 summarizes the resulting correlation coefficients r_Q and p-values for the four test images in Figures 1-4. It appears from the table that the p-values yield high values approximate to unity for resembled images, either uniform or complicated images, and low values close to zero for dissimilar images. The correlation coefficient r_Q cannot generate discriminating values for dissimilar images such as the ones shown in Figures 2 and 4. To further compare the detection effectiveness of the similarity measures of Q-Q plots and the traditional pattern matching, Table 1 also lists the NCC values for the four test samples in their original 2D gray-level images. Figures 1 and 4 reveal that NCCs cannot reliably discriminate the difference between faultless and defective images. These results suggest that the p-value of Q-Q plots should be used as the similarity measure for template-based defect detection.

In order to reduce the effect of shifting due to minor misalignment or process variation in manufacturing, only the gray levels of edge pixels in the compared images are used for the construction of Q-Q plots. In this study, the edge pixels are defined by those that have Sobel gradients larger than the mean gradient of the image. Since the proposed template matching scheme is based on quantiles, the extracted numbers of edge pixels in the template and inspection images need not be equal.

As mentioned in previous experiments, the p-value is highly responsive to subtle defects in an inspection image, and is an excellent similarity measure for defect detection in terms of the discrimination capability. However, the drawback of the

p-value measure is its sensitivity to lighting. An illumination change will cause the resulting Q-Q plot of two resembled images to deviate from the 45° reference line, and yield a small p-value close to zero. In order to make the p-value a practical similarity measure for defect detection, an affine transformation is carried out in the Q-Q plot to normalize the points of paired quantiles. The normalization process brings the paired points in the Q-Q plot to lie on the 45° reference line for two resembled images, while preserving the nonlinear shape of the Q-Q plot for two dissimilar images.

Let $l^T = a \cdot l^I + b$ be the estimated line equation for the data sets of points $\left\{\left(l_k^I, l_k^T\right)\right\}_{k=1}^K$. The slope a and intercept b of the regression line can be easily calculated using the least-squares method. The coordinates of a paired point (l_k^I, l_k^T) can then be normalized by

$$\begin{bmatrix} \hat{l}_k^I \\ \hat{l}_k^T \end{bmatrix} = \begin{bmatrix} \cos\Delta\theta & -\sin\Delta\theta \\ \sin\Delta\theta & \cos\Delta\theta \end{bmatrix} \begin{bmatrix} l_k^I \\ l_k^T - b \end{bmatrix}$$

where $\Delta\theta$ is the angular difference between the estimated regression line and the 45° reference line, i.e., $\Delta\theta = \frac{\pi}{4} - \tan^{-1} a$.

Figures 5 and 6 illustrate faultless and defective images, respectively, under overexposure and underexposure conditions. For the faultless image in Figure 5, the resulting graphs in the Q-Q plots are approximately linear, but depart from the 45° reference line for the overexposed and underexposed images. The normalized points in the Q-Q plots lie fairly well on the 45° reference line, and result in high

p-values of 0.99, as seen in Table 2. For the defective images in Figure 6, the normalized graphs in the Q-Q plots remain curve-shaped, and the resulting p-values are as small as 0.0001. The results reveal that the p-value of the normalized Q-Q plots can tolerate illumination changes for faultless images, and yet well preserves nonlinearity of the graphs in the plots for defective images.

3. EXPERIMENTAL RESULTS

In this section, we present the experimental results for evaluating the efficacy of the proposed Q-Q plot based pattern matching scheme for defect detection. In our implementations, all algorithms were programmed in the C++ language and executed on a personal computer with a Pentium 4, 1.9 GHz processor. The effective image size is 400×400 pixels with eight-bit gray levels.

In order to visualize the detection results of two compared images, the resultant p-values are represented as an intensity function by linearly scaling up to 255 in an 8-bit display (i.e., $p \cdot 255$). The brightness of each pixel is, therefore, proportional to the magnitude of p-value. The darker the intensity in the resulting image, the stronger the evidence of a defect.

3.1 The effect of window size

Using the template-based matching technique for defect inspection, one has to calculate the similarity measure of each pixel defined in a small neighborhood window. An overly small size of the window will generate much noise in the

detection image, whereas an overly large size of the window may smooth out subtle defects. Figures 7(a) and (b) show two compared images of PCB surfaces. The resulting p-values as an intensity function from window sizes 15×15, 20×20, 30×30 and 45×45 pixels are respectively presented in Figures 7(c)-(f). A few noisy points appear in the detection image with the small window size of 15×15. A window size of 30×30 or larger well detects the defect without presenting noise. The computation times for window sizes 20×20, 30×30 and 45×45 pixels are 0.28, 0.30 and 0.32 seconds, respectively. They indicate that the proposed Q-Q plot based template matching is nearly invariant to the increased size of a neighborhood window. Also notice that the detection results in Figures 7(c)-(f) visibly look like binary images due to the high discrimination capability of the proposed similarity measure of p-value (i.e., p-value is approximately unity for resembled regions, and zero for dissimilar regions).

For the sake of comparison, the detection results of Figures 7(a) vs. (b) using the traditional NCC in 2D gray-level images are also demonstrated in Figures 8(a)-(d), in which only nonnegative NCC values are considered and transformed as an intensity function of an 8-bit display, i.e., $\max\{0, \text{NCC}\}\cdot255$. The results show that the NCC method may detect defect regions along with many false-alarmed areas. The discrimination capability of the traditional NCCs is not as good as the proposed p-value of Q-Q plots. Computation time of the NCC method dramatically increases from 1.37 seconds with a small window of size 20×20 pixels, to 5.87 seconds with a large window of size 45×45 pixels. In the following subsequent experiments, a window size of 30×30 pixels is employed for all test samples.

In defect detection applications, the computational complexity of the

traditional NCC in a 2D image is $O(m \cdot n \cdot M \cdot N)$ for an image of size $M \times N$ and a template window of size $m \times n$. The computational complexity of the proposed Q-Q plot scheme can be efficiently reduced to $O(K \cdot M \cdot N)$, where K is the number of paired quantiles in the Q-Q plot. The value of K is generally very small. For a percentage step of 5% (i.e., Δq=0.05), K is only 20. Given a template window of size 30×30, the value of $m \times n$ is then 900. Note that the computational complexity of the proposed method is relatively invariant to the template window size $m \times n$.

3.2 The effect of shifting

In the previous section, we have suggested the use of gray levels of edge pixels to construct the Q-Q plot so that the noise due to the minor shifting can be alleviated. To further reduce the effect of shifting, which is a common problem in template-based defect inspection, a search procedure is carried out in a small neighborhood for those pixels that have a small p-value. That is

$$p(x,y) = \max\{p(x+i, y+j),\ -W \le i, j \le W\},\ \ \forall p(x,y) < T_p$$

where $p(x,y)$ is the p-value at pixel coordinates (x,y); the integer W defines the search neighborhood of size $(2W+1)\times(2W+1)$; and T_P is a predetermined threshold of p-value. In this study, we use a small search neighborhood of 3×3, i.e., the 8 adjacent neighbors of (x, y) with W=1. Since the p-value is generally very small for dissimilar images, the p-value threshold T_P is conservatively selected to be 0.3. Note that the search procedure is only required for the potential defect pixels with low p-values. Figure 9(a) shows the template image of a test sample for evaluating the effect of shifting. Figures 9(b) and (c) are a faultless version and a defective version (missing components marked with a dotted square) of the test sample. These

inspection images were horizontally shifted to the right by three pixels. The detection results of the proposed method with and without the use of the search procedure are illustrated in Figures 9(d)-(g). The results reveal that the proposed method can tolerate minor changes of shifting. With the aid of the search procedure, noisy points can be effectively eliminated without increasing much computational load.

3.3 The effect of lighting and more detection results

To demonstrate the effect of varying illumination, Figure 10(a) shows a PCB template image under a normal illumination. Figure 10(b) is a defective version of the PCB under the same illumination, in which two missing components are marked with a dotted circle. Figures 10(c) and (d) further show underexposed and overexposed versions of the defect sample in Figure 10(b). The detection results shown in Figures 10(e)-(g) indicate that the p-values of the normalized Q-Q plots can reliably detect defects for moderate variations of illumination.

Figures 11(a1)-(a4) show four additional test images of various PCB samples under the same parameter setup suggested in this study. Figure 11(b1) presents an IC image with blurred printed characters, Figure 11(b2) involves a contaminated defect, Figure 11(b3) contains a misaligned component, and Figure 11(b4) includes a deformed component. The detection results as displayed by $p \cdot 255$ in Figures 11(c1)-(c4) have shown the effectiveness of the proposed method for detecting subtle defects embedded in complicated gray-level images.

Figures 12(a1) and (a2) demonstrate two IC wafer images, and Figures 12(a3) and (a4) present two LCD panel images for further testing the generality of the

proposed method in template-based defect detection. Figures 12(b1)-(b4) are the defective versions of the templates in Figures 12(a1)-(a4), respectively. The experimental results in Figures 12(c1)-(c4) show that the defect areas as displayed by $p \cdot 255$ are notably detected and located. Approximately black areas associated with the defects and a white background for the clear region are generated in each of the resulting images.

4. CONCLUSIONS

In this study, we have proposed a quantile-quantile plot based pattern matching scheme for defect detection. In the Q-Q plot, the quantiles of an inspection image are plotted against the corresponding quantiles of the template image. If both images are exactly the same, each pair of the corresponding quantiles will lie on a straight line with slope 1 through the origin. The graph in the plot will depart from the 45° reference line or become curve-shaped for two dissimilar images. The p-value of Chi-square test is adopted as a measure of straightness (i.e. similarity) for points of paired quantiles in the Q-Q plot.

With a proper affine transformation that normalizes the points of paired quantiles with a desired slope of 1 and intercept of 0 in the Q-Q plot, the p-value measure can tolerate moderate changes of illumination. Compared with the traditional NCC methods, the proposed Q-Q plot based template matching scheme is computationally efficient. It is nearly invariant to the size of the neighborhood window and, therefore, a user can select a proper window size to maximize the detection effectiveness for the

object under inspection without trading off the computational efficiency. The proposed method provides an effective and efficient referential approach for industrial inspection of defects in complicated gray-level images.

The experimental results have shown that the proposed method can be used for a variety of industrial inspection applications as long as the templates are available. The proposed Q-Q plot based template matching scheme can also be applied for object recognition where an instance of a small reference template must be detected in a large scene image. By sliding the template window pixel by pixel over the entire image, the maximum values or peaks of the resultant p-values indicate the matches between the template and subimages in the scene. In this study, the Q-Q plot based defect detection scheme is mainly applied to gray-level images. Since a color image can provide more cues for discriminating anomalies and many defects of industrial products may result from faulty color, the Q-Q plot that uses the tristimulus color values of R (red), G (green) and B (blue) for defect detection in color images is worth to investigate in the future.

REFERENCES

Bonmassar, G., Schwartz, E. L., 1998. Improved cross-correlation for template matching on the Laplacian pyramid. Pattern Recognition Letters 19, 765-770.

Brunelli, R., Poggio, T., 1993. Face recognition: features versus templates. IEEE Trans. Pattern Anal. Machine Intell. 15, 1042-1052.

Cai, X. Y., Kvasnik, F., Blore, R. W., 1994. Wafer fault measurement by coherent optical processor. Applied Optics 33, 4487-4496.

Chang, M.-C., Fuh, C.-S., Chen, H.-Y., 2001. Fast search algorithms for industrial inspection. International Journal of Pattern Recognition and Artificial Intelligence 15, 675-690.

Costa, C. E., Petrou, M., 2000. Automatic registration of ceramic tiles for the purpose of fault detection. Machine Vision and Applications 11, 225-230.

Gallegos, J. M., Villalobos, J. R., Carrillo, G., Cabrera, S. D., 1996. Reduced-dimension and wavelet processing of SMD images for real-time inspection. In: Proceedings of the IEEE Southwest Symposium on Image Analysis and Interpretation, San Antonio, TX, pp. 30-36.

Gross, A. D., Rosenfeld, A., 1987. Multiresolution object detection and delineation. Computer Vision Graph. Image Process. 39, 102-115.

Grudin, M. A., 2000. On internal representations in face recognition systems. Pattern Recognition 33, 1161-1177.

Kim, J. H., Cho, H. S., Kim, S., 1996. Pattern classification of solder joint images using a correlation neural network. Engineering Applications of Artificial Intelligence 9, 655-669.

Levine, D. M., Ramsey, P. P., Smidt, R. K., 2001. Applied Statistics for Engineers and Scientists. Prentice-Hall, Upper Saddle River, NJ.

Lewis, J. P., 2003. Fast normalized cross-correlation. Available from:

<www.idiom.com/~zilla/Work/nvisionInterface/nip.pdf>

NIST/SEMA TECH, 2004. Quantile-quantile plot. e-Handbook of Statistical Methods. Available from: <www.itl.nist.gov/div898/handbook/eda/section3/qqplot.htm>

Ooi, J., Rao, K., 1991. New insights into correlation-based template matching. In: Proceedings of SPIE, V. 1468, Applications of Artificial Intelligence IX, Orland, FL., pp. 740-751.

Penz, H., Bajla, I., Mayer, K., Krattenthaler, W., 1999. High speed template matching with point correlation in image pyramids. In: Proceedings of SPIE, V. 3827, Bellingham, WA, pp. 85-94.

Ratan, A. L., Grimson, W. E. L., Wells, W. M. III, 2000. Object detection and localization by dynamic template warping. International Journal of Computer Vision 36, 131-147.

Tsai, D.-M., Chiang, C.-H., 2002. Rotation-invariant pattern matching using wavelet decomposition. Pattern Recognition Letters 23, 191-201.

Tsai, D.-M., Lin, C.-T., 2003. Fast normalized cross correlation for defect detection. Pattern Recognition Letters 24, 2625-2631.

Tsai, D.-M., Lin, C.-T., Chen, J. F., 2003. The evaluation of normalized cross correlations for defect detection. Pattern Recognition Letters 24, 2525-2535.

Tsai, D.-M., Tsai, Y.-H., 2002. Rotation-invariant pattern matching with color ring-projection. Pattern Recognition 35, 131-141.

UCLA, 2003. Statistical Computing Resources. Available from: <www.ats.ucla.edu/stat>

Yazdi, H. R., King, T. G., 1998. Application of ‘vision in the loop’ for inspection of lace fabric. Real-Time Imaging 4, 317-332.

Figure

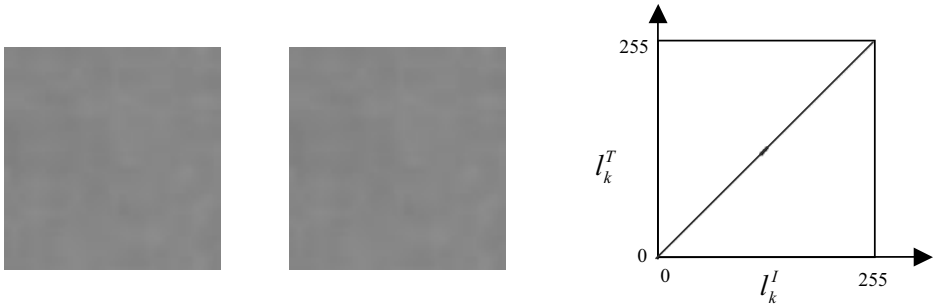

(a) (b) (c)

Figure 1. Q-Q plot for two uniform images.

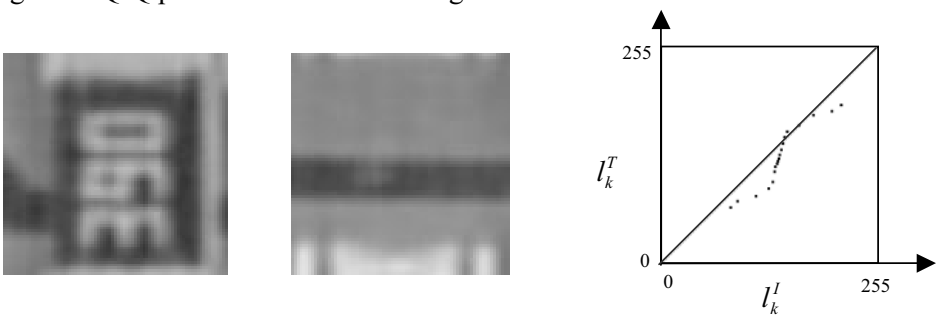

(a) (b) (c)

Figure 2. Q-Q plot for two heterogeneous images.

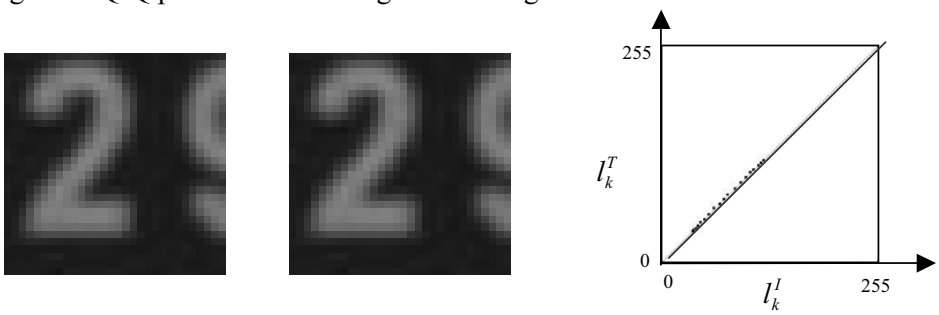

(a) (b) (c)

Figure 3. Q-Q plot for two faultless printed-character images.

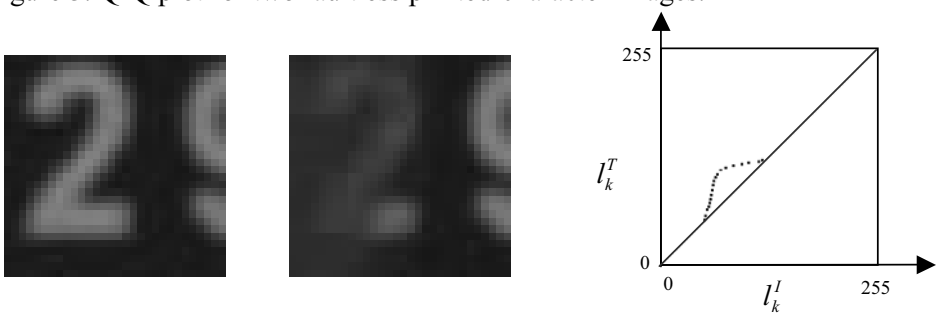

(a) (b) (c)

Figure 4. Q-Q plot for the faultless printed-character image and a blurred version of the sample.

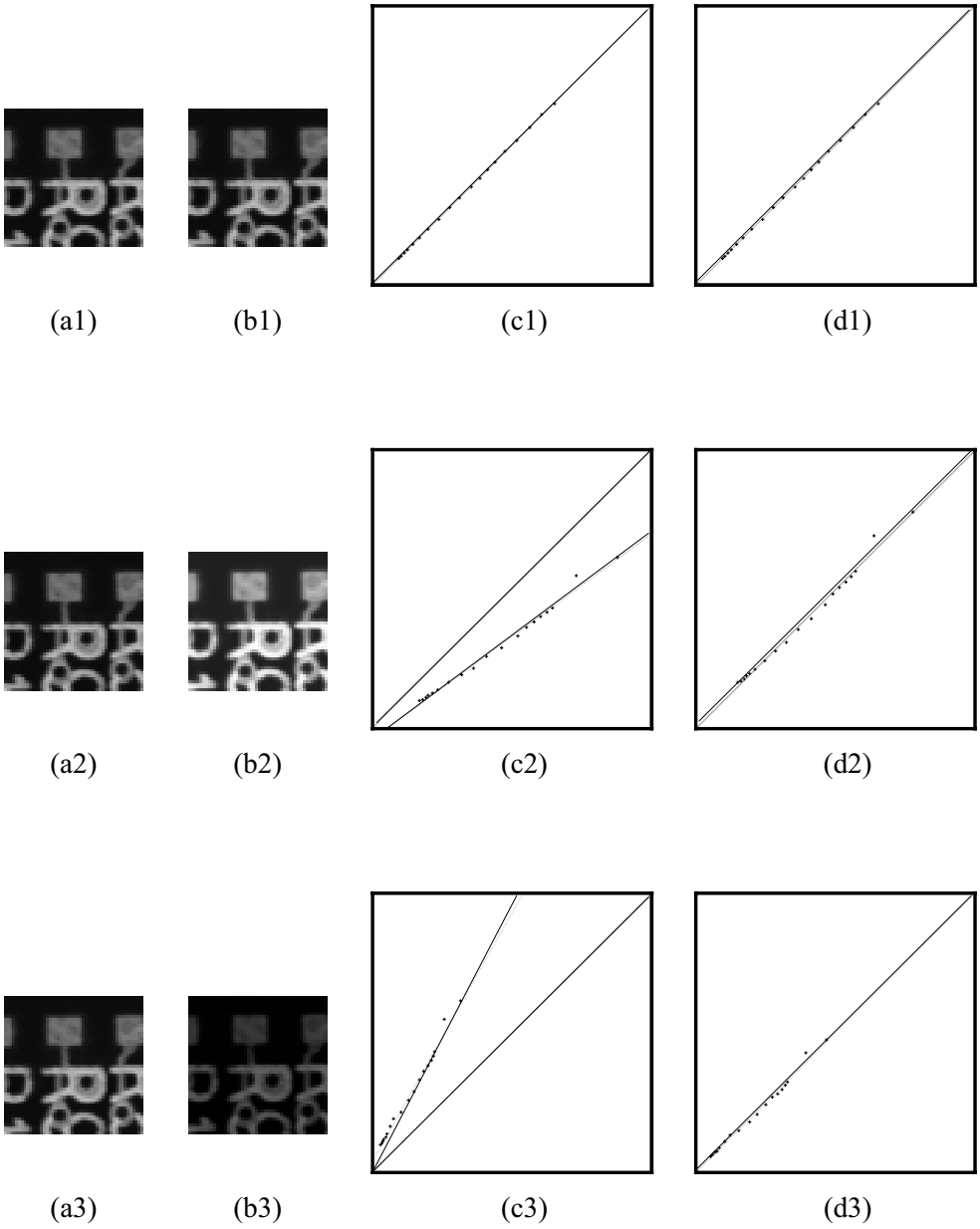

Figure 5. (a1)-(a3) The template image ; (b1)-(b3) Faultless test images under normal lighting, overexposure and underexposure conditions, respectively; (c1)-(c3) the corresponding Q-Q plots prior to normalization ; (d1)-(d3) the resulting Q-Q plots after normalization.

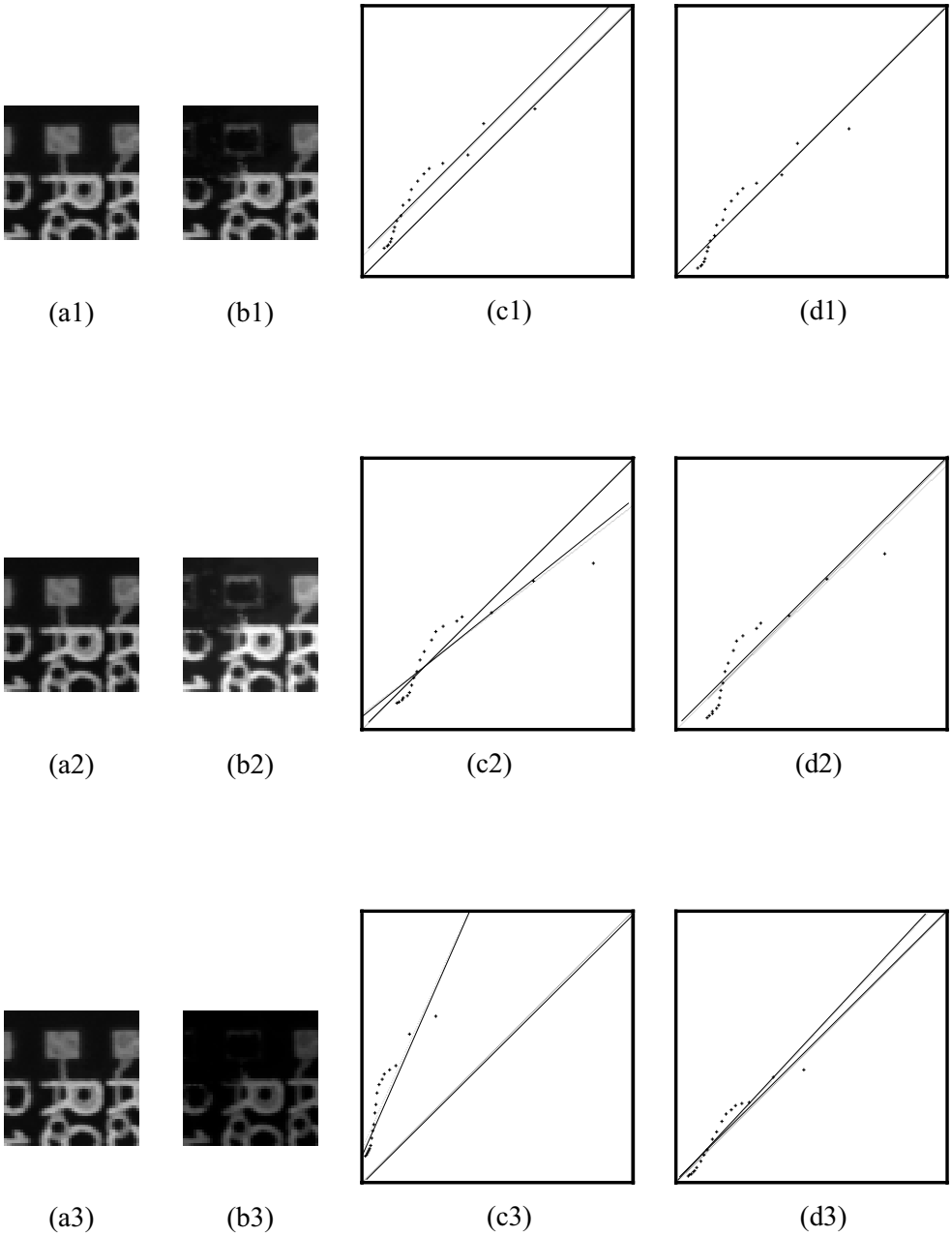

Figure 6. (a1)-(a3) The template image; (b1)-(b3) Defective test images under normal lighting, overexposure and underexposure conditions, respectively; (c1)-(c3) the corresponding Q-Q plots prior to normalization; (d1)-(d3) the resulting Q-Q plots after normalization.

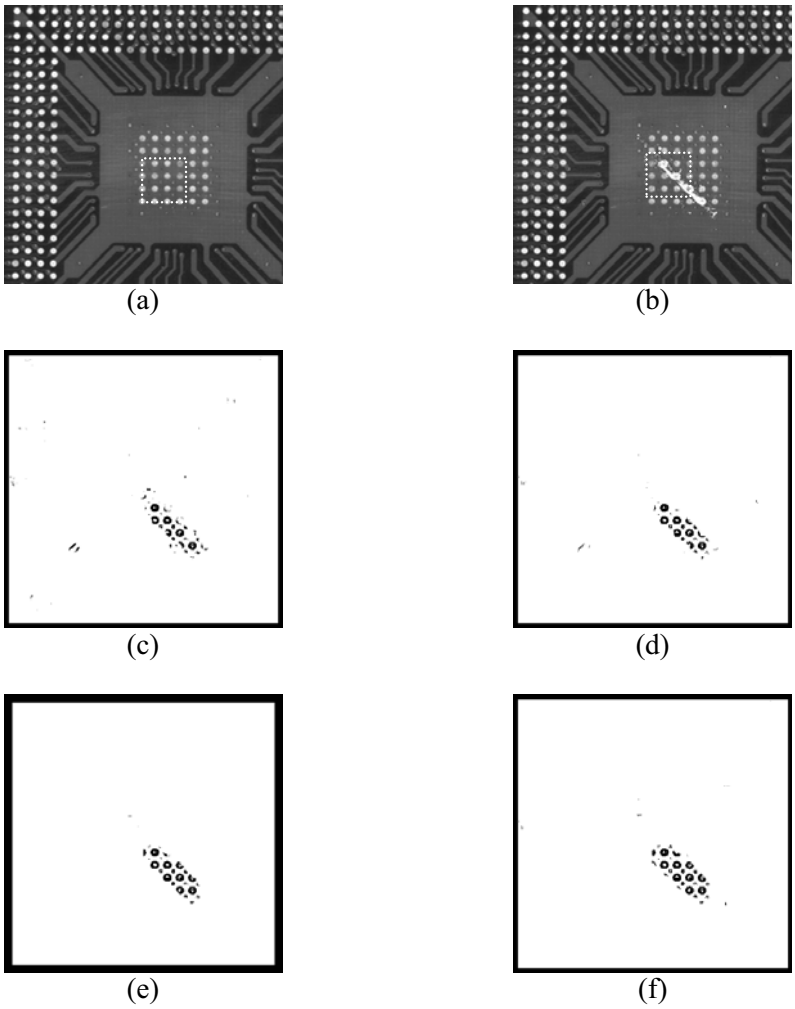

Figure 7. The effect of changes in windows size: (a) the template image; (b) the inspection image involving a defect; (c)-(f) detection results from window size of 15×15, 20×20, 30×30 and 45×45 pixels, respectively.

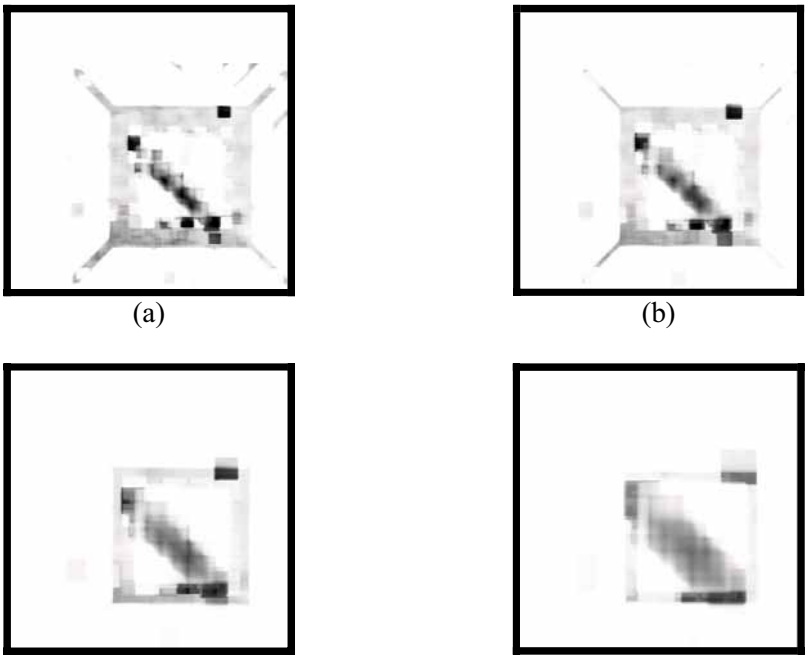

(a) (b) (c) (d)

Figure 8. The effect of changes in window size for the test images in Figure 7 (a) and (b) using the traditional NCC: (a)-(d) detection results from window size of 15×15, 20×20, 30×30 and 45×45 pixels, respectively.

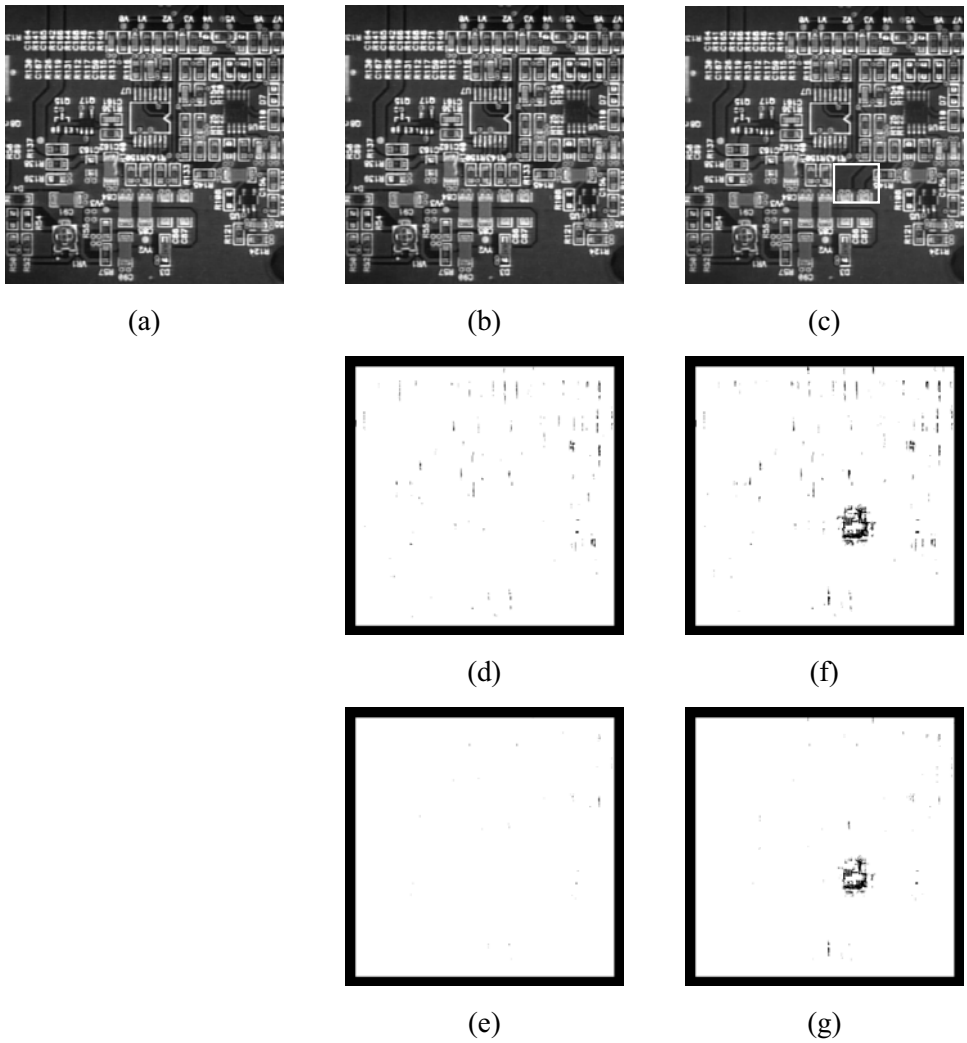

Figure 9. The effect of shifting: (a) the template image; (b) the faultless inspection image; (c) the inspection image containing missing components (as marked with a dotted square); (d), (e) the detection results for the inspection image in (b) without and with the use of the search procedure; (f), (g) the detection results for the inspection image in (c) without and with the use of the search procedure.

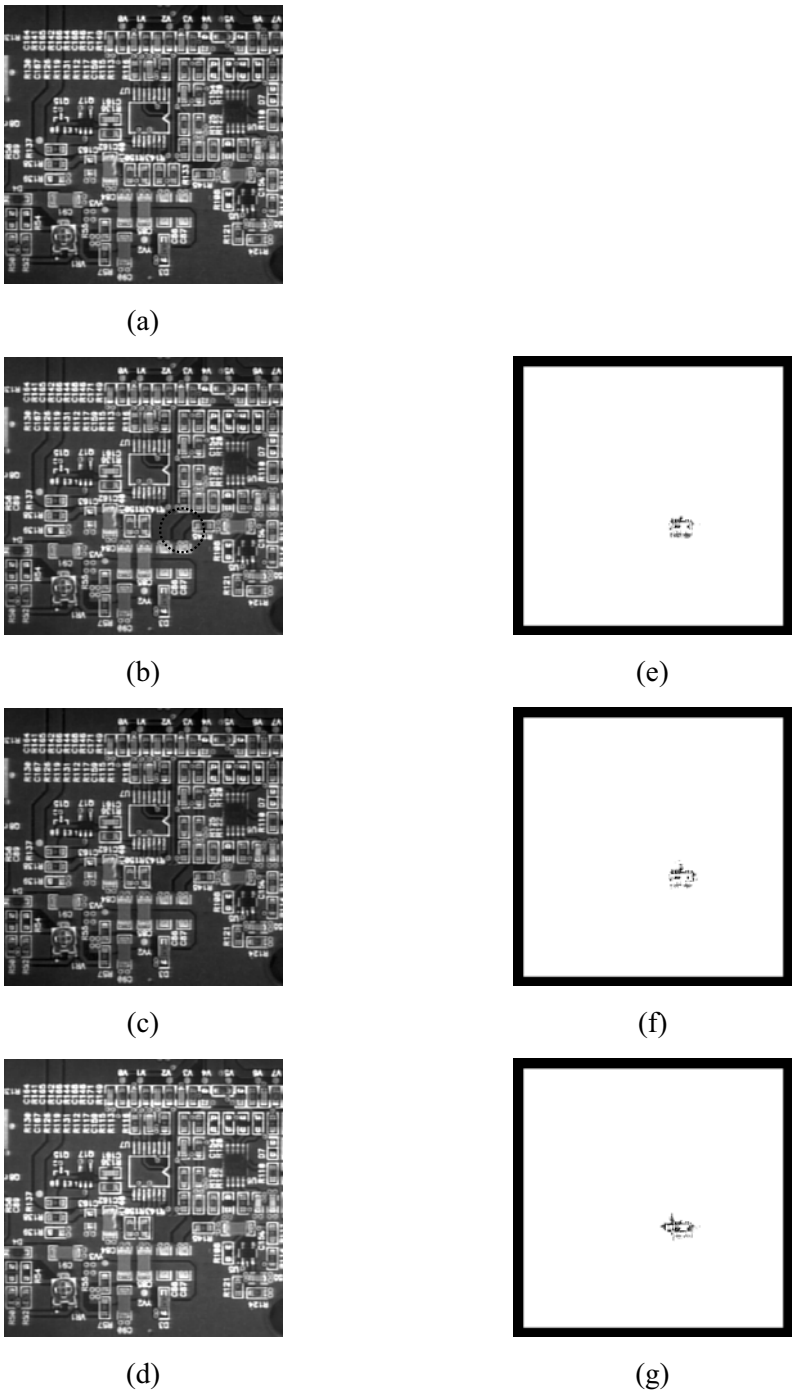

Figure 10. The effect of illumination changes: (a) the template image; (b) a defect image under the same illumination as (a); (c), (d) underexposed and overexposed versions of the defect image in (b); (e)-(g) the detection results of (b), (c) and (d),respectively, based on the p-value in the normalized Q-Q plots.

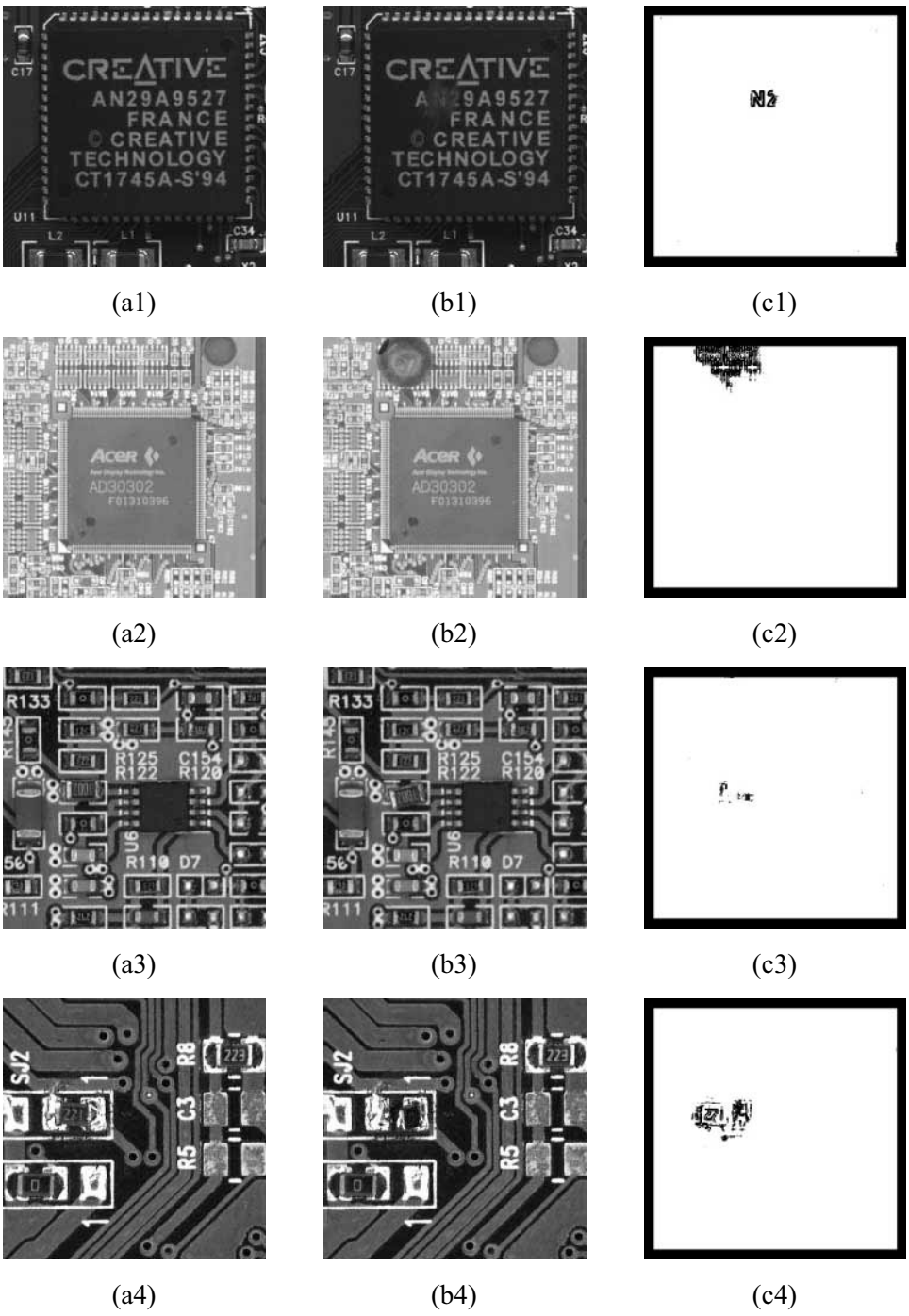

(a1) (b1) (c1)

(a2) (b2) (c2)

(a3) (b3) (c3)

(a4) (b4) (c4)

Figure 11. Defect detection in four assembled PCBs: (a1)-(a4) The template images; (b1)-(b4) the inspection images that contain various defects; (c1)-(c4) the respective detection results of (b1)-(b4).

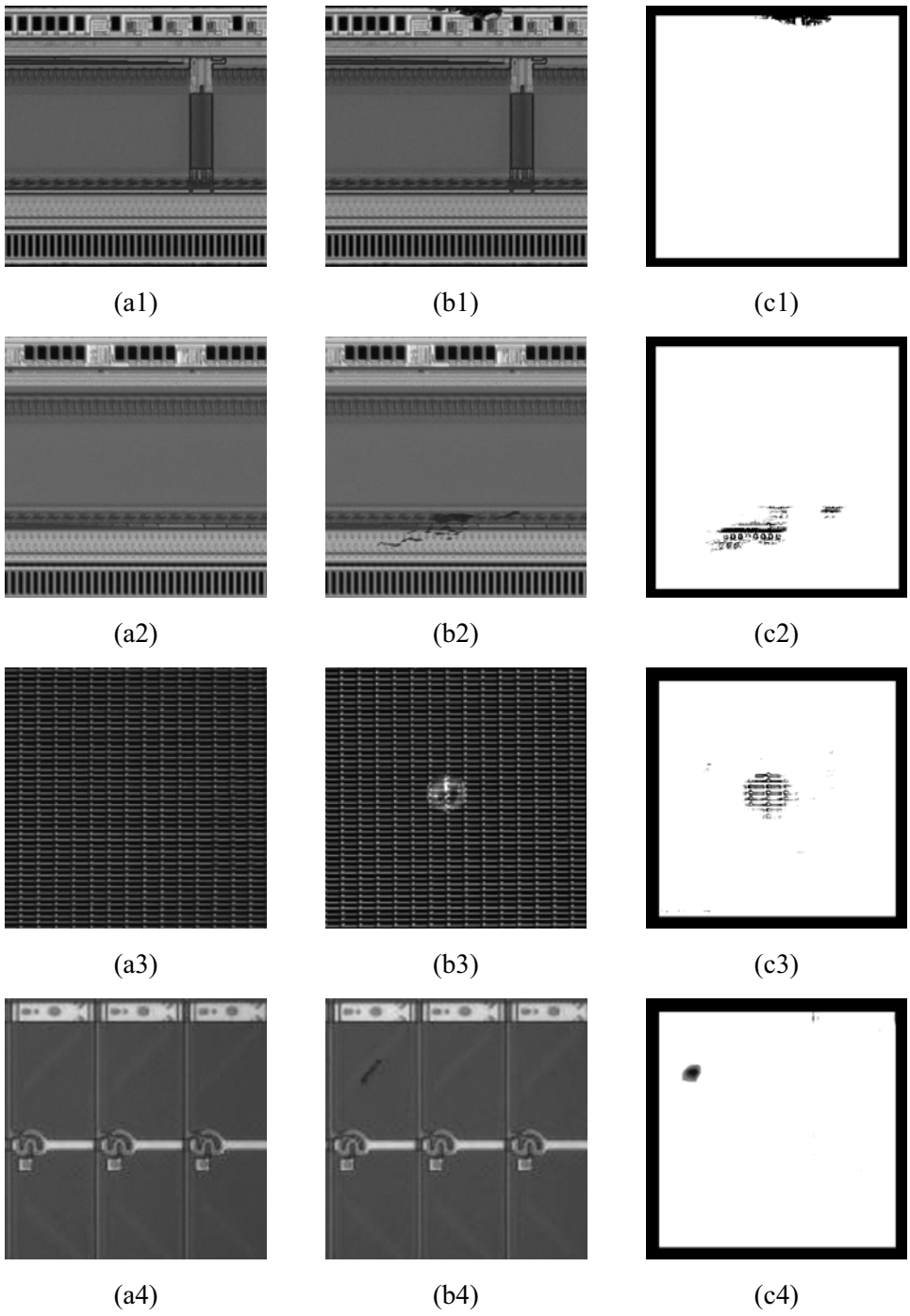

Figure 12. Defect detection in IC wafers ((a1) and (a2)) and LCD panels ((a3) and (a4)): (a1)-(a4) The template images; (b1)-(b4) the inspection images that contain various defects; (c1)-(c4) the respective detection results of (b1)-(b4).

Table

Table 1. Comparison of similarity measures for the test images in Figures 1-4.

Test image	Q-Q plot		Traditional NCC
	p-value	r_Q	
Figure 1	0.99	0.99	0.72
Figure 2	0.01	0.83	0.65
Figure 3	0.99	0.99	0.99
Figure 4	0.01	0.82	0.77

Table 2. The resulting p-values with and without the normalization for the Q-Q plots in Figures 5 and 6.

Test Image		P-value		Estimated direction(dgs.)	
		Original	Normalized	Original	Normalized
Faultless images (Fig. 5)	Normal lighting(Fig.5(b1))	0.9999	0.9999	45.0	45.0
	Overexposure (Fig.5(b2))	0.0001	0.9990	36.0	44.9
	Underexposure(Fig.5(b3))	0.0001	0.9991	61.7	45.2
Defective images (Fig. 6)	Normal lighting(Fig.6(b1))	0.0001	0.0001	45.1	45.1
	Overexposure (Fig.6(b2))	0.0001	0.0001	35.3	44.5
	Underexposure (Fig.6(b3))	0.0001	0.0001	60.3	45.9

Responses to reviewer 1

Responses to the comments of reviewer 1:

1. Computational complexity of the proposed method vs. the traditional NCC method has been discussed on page 13 (the first paragraph) in the revised manuscript.

2 & 3. Besides the PCB test samples (Figure 11), we have included two IC wafer images (Figures 12(a1) and (a2)), and two LCD (Liquid Crystal Display) panel images (Figures 12(a3) and (a4)) in the revision to show the performance of the proposed method in other applications. The potential applications of the proposed method have also been discussed in the conclusion section (2nd paragraph, page 16) in the revised manuscript.

4. The future research direction has been included in the conclusion section (2nd paragraph, page 16) in the revised manuscript.

Responses to reviewer 2

Responses to the comments of reviewer 2:

1. Eq. (1) is a general description for any continuous data set. Since *F(x)* is a cumulative density function for continuous random variables, it is continuous and strictly increasing. $F(x_q) = q$ and $x_q = F^{-1}(q)$ can be uniquely defined for continuous data sets. The discrete version of *F(x)* used for digital images in this study is given in eqs. (6) and (7). The discussion above has been included on pages 3 and 4 (the last paragraph on page 3, and the first paragraph on page 4) in the revised manuscript.

2. $F_T^{-1}(q_i)$ in eq. (3) has been corrected as $F_I^{-1}(q_i)$.

3. The typing mistake "pot" (page 7, the first line of section 2.2) has been corrected as "plot" in the revision.

4. - When the correlation coefficient r_Q eq. (8) is close to -1, it indicates a reversal of intensities between two compared images. In this case, the corresponding area should be identified as a fault in the defect detection application. In this study, r_Q value is linearly converted to an 8-bit intensity function (i.e., r_Q x 255) so that the defective areas can be visually observed in the resulting image. Since a negative value of r_Q shows a strong evidence of defect, we simply set the negative r_Q to zero, and display an intensity of zero (i.e., a black pixel) in the resulting image. The clarification of r_Q is given on page 8 (the first paragraph).
   - Since the correlation coefficient is a commonly used metric to evaluate the linearity of the resulting shape in the Q-Q plot, we retain it in this paper for interested readers.
   - The word "discriminatability" has been changed to "discrimination capability" in the revised manuscript.

5 & 6. Given an observed data set $\{x_1, x_2, ..., x_n\}$, the Chi-square statistic is defined by

$$\chi^2 = \sum_{i=1}^{n} (x_i - \mu)^2 \Big/ \sigma^2$$

if $x_i's$ are normally distributed with mean μ and standard deviation σ. If the distribution is unknown, χ^2 can be calculated by

$$\chi^2 = \sum_{i=1}^{n} (x_i - E_i)^2 \Big/ E_i^2$$

where E_i is the expected value associated with x_i.

The computation of the p-value in eqs. (9)-(10) is reformulated, and the Gamma function is clearly defined in eq. (11) for better understanding. The clarification of the Chi-square statistic and the p-value is given on page 8 in the revision.

7. The typing mistake "Theses results" has been corrected in the revision (page 9, line 10 of paragraph 2).

8. The conventional form of a line function has been used in the revised manuscript (2nd paragraph, page 10).

9. The symbol *N(x,y)* used for representing a search neighborhood has been discarded, and improved with a simpler and clearer representation (see the equation and description on page 13).

10 & 11. The web sites for references (Lewis, J. P., 2003) and (UCLA, 2003) have been verified and corrected.